Design and Construction

Comparative Study on Restraining Systems of Self-Anchored Suspension Bridges

Changyan Niu *, Yongcheng Lu and Jianguo Dai

Shanghai Municipal Engineering Design Institute (Group) Co., Ltd., Shanghai 200092, China.
* Correspondence: niuchangyan@smedi.com

Abstract: Using a practical engineering project as an example, this study analyzes a self-anchored suspension bridge under two different restraining systems: a fully floating system and a semi-floating system. This investigation focuses on static performance, overall stability, wind resistance, and seismic behavior. The static characteristics and dynamic responses of the self-anchored suspension bridge under different restraining systems are obtained, and the influence of the tower–girder constraint conditions on the mechanical behavior of the structure is discussed.

Keywords: self-anchored suspension bridge; fully floating system; semi-floating system; static characteristics; dynamic response

1   Introduction

In the field of long-span bridges, suspension bridges have long been regarded as one of the most critical structural forms. In recent years, the rapid development of urban bridge construction has led to an increased use of self-anchored suspension bridges. This type of bridge has gradually become a preferred option in urban bridge design because of its remarkable aesthetic appeal, excellent spanning capability, and relatively high adaptability to diverse geological conditions [1–3]. However, as the technology of self-anchored suspension bridges continues to advance, the challenges associated with their static stability and dynamic performance in large-span applications have become increasingly prominent.

Extensive research has been conducted both domestically and internationally on the static characteristics and seismic performance of traditional long-span suspension bridges [4–9]. Hu et al. [3], taking the Jiangyin Yangtze River Bridge as a case study, constructed a dynamic time-history analysis model to investigate the longitudinal seismic response characteristics of the bridge. Huang [4] selected another Yangtze River Bridge project to analyze the underlying mechanisms of seismic traveling wave effects in depth. Li [5] focused on the influence of pile–soil interactions on the natural frequency of pedestrian suspension bridges while also examining the impact of the seismic input direction on the results of time-history analysis. These studies have shown that the design parameters and boundary conditions of conventional suspension bridges significantly affect their overall mechanical performance.

Owing to the relatively late development of self-anchored suspension bridges, research on the influence of restraining systems on their static and seismic performance remains limited both in China and abroad. In this study, on the basis of a practical engineering project, a finite element model is established to analyze the static and dynamic characteristics of a self-anchored suspension bridge. The static behavior and dynamic response under different tower–girder restraining systems are obtained, and the influence of the tower–girder constraint conditions on the mechanical performance of the bridge is investigated.

2 Project Overview

The project is a three-span self-anchored suspension bridge (Figure 1) with a span arrangement of (130 + 336 + 130) m. The main girder adopts a twin-edge steel box girder section, and the main towers are of the portal-frame type. The tower foundations consist of bored cast-in-place piles with a diameter of 2.0 m. The main bridge features a full-width deck layout, accommodating six traffic lanes (three in each direction) and nonmotorized lanes on both sides. Hangers are arranged in both the main span and side spans. The main cable of the central span has a sag-to-span ratio of 1/5.17. The two main cables are arranged in parallel planes, with a transverse spacing of 26.6 m and a longitudinal spacing of 12.0 m between adjacent hangers.
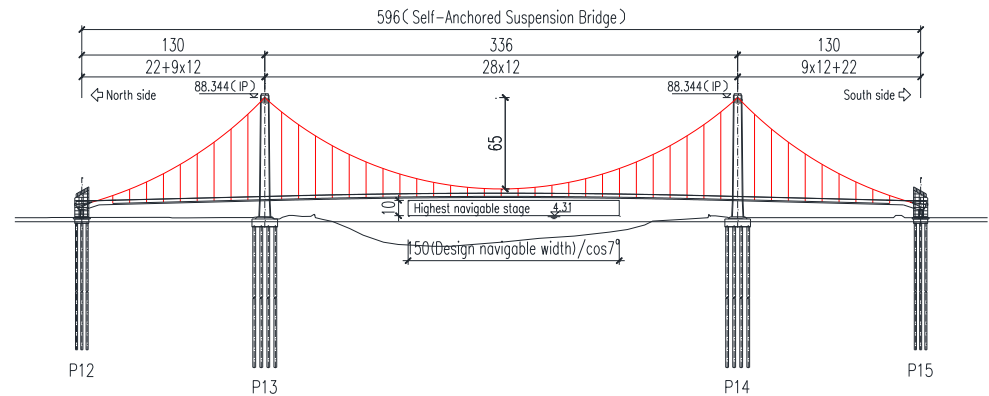

Figure 1 Bridge layout diagram (unit: m)

3 Comparison of Restraining Systems

To determine the most suitable vertical restraint form for the main girder of the bridge, a comparison of the vertical restraint forms at the tower–girder junction was conducted. The commonly used vertical restraint forms for the main girder include the fully floating system (Figure 2) and the semi-floating system (Figure 3). In the fully floating system, no vertical support is provided at the tower–girder junction, whereas in the semi-floating system, vertical support is provided at the junction.
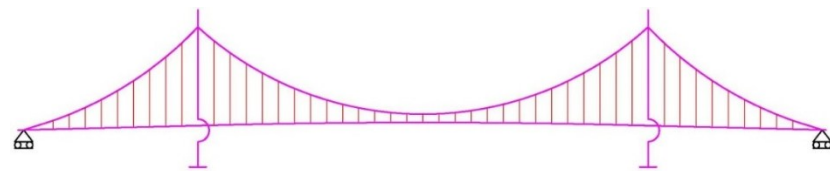

Figure 2 Schematic diagram of the fully floating system for self-anchored suspension bridge
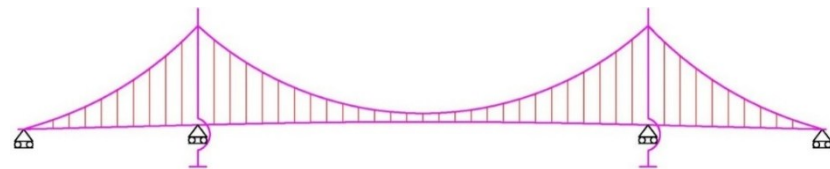

Figure 3 Schematic diagram of the semi-floating system for self-anchored suspension bridge

3.1 Influence of Tower–Girder Restraint on the Static Characteristics of a Self-Anchored Suspension Bridge

A full bridge finite element model was established using Midas Civil (Figure 4) to analyze the two restraint forms, namely, the fully floating system and the semi-floating system. The main cables and hangers are modeled using elastic cable elements, whereas the main girder, tower, and bridge piers are modeled using beam elements. The main cables are connected to the top of the tower, and the anchorage points to the main girder are connected via master–slave restraints. The main girder is constrained for single-sided transverse displacement at the tower (and vertical

displacement at the main tower for the semi-floating system), whereas vertical and single-sided transverse displacements are constrained at the pier ends. The tower base and pier bases are fixed.
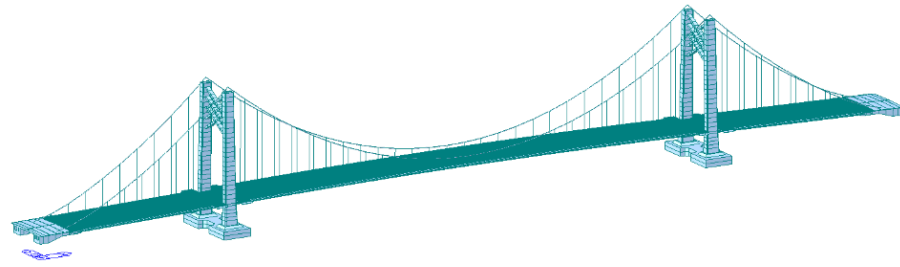

Figure 4 Spatial beam–element calculation model

3.1.1 Live Load Bending Moment and Deflection of the Main Girder

The self-anchored suspension bridge model was analyzed under two different tower–girder restraint conditions. The resulting live load bending moments of the main girder are shown in Figure 5. The vehicle load corresponds to Highway Class I, with six traffic lanes in both directions. The relevant parameters are adopted in accordance with the "General Code for Design of Highway Bridges and Culverts" [10].
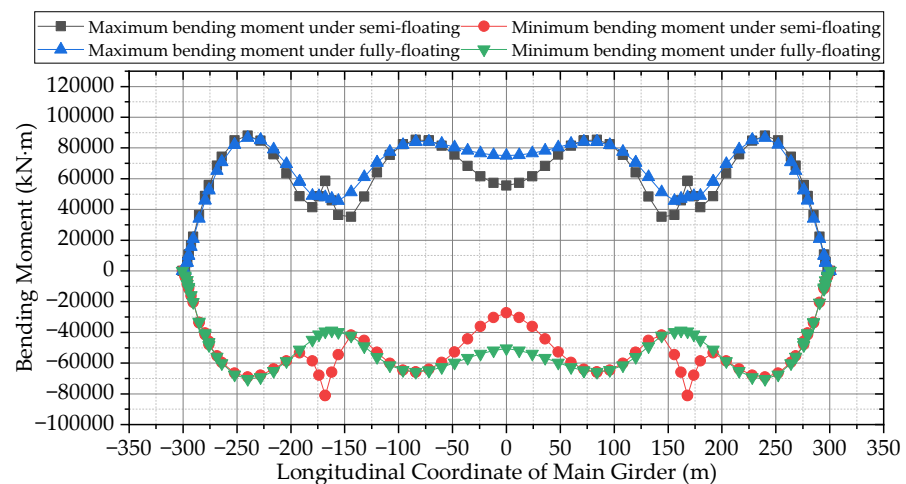

Figure 5 Live load bending moment diagrams of main girder under two restraint systems
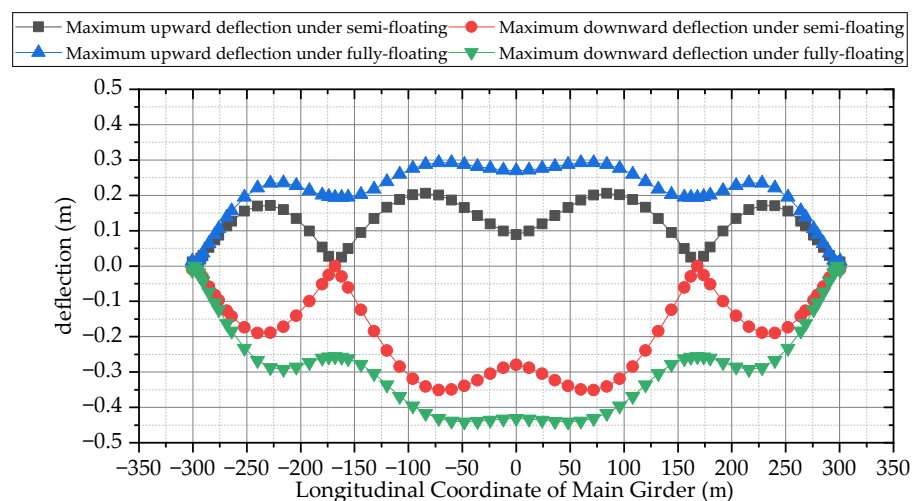

Figure 6 Live load deflection diagrams of main girder under two restraint systems

As shown in Figure 5, the live load bending moment envelopes are generally similar across most regions of the bridge. The tower–girder restraint primarily affects the local bending moment near the supports, with the semi-floating system exhibiting significantly larger bending moments at the girder supports. Figure 6 indicates that the maximum live load deflection of the main girder under the semi-floating system is 0.351 m, whereas that under the fully floating system is 0.441 m. Both values satisfy the requirements of the relevant design code. Although the two systems have a certain influence on the live load deflection, the overall impact is limited.

3.1.2   Overall Structural Stability of the Bridge

A comparison of the global buckling modes under the two restraint systems reveals that, in both cases, the first buckling mode corresponds to the instability of the main towers (Figure 7). The overall stability analysis results indicate that the first-order stability coefficient is 15.3 for the semi-floating system and 13.2 for the fully floating system, with only a slight difference between the two.
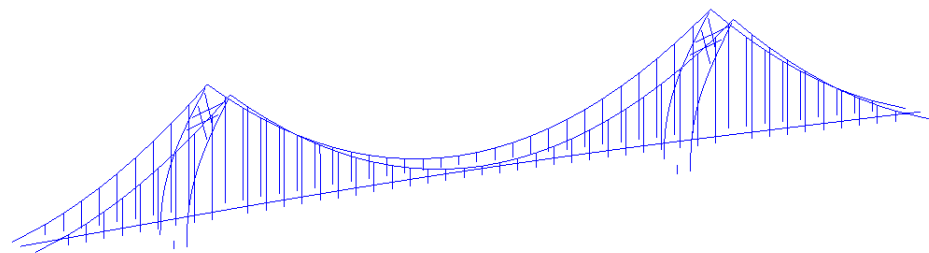

Figure 7   First-order buckling mode

3.2   *Influence of Tower–Girder Restraint on the Wind Resistance Performance of Self-Anchored Suspension Bridges*

The comparison focuses primarily on the flutter stability performance of the bridge under both restraint systems in the completed and construction stages. The flutter critical wind speed V_{cr} is calculated with reference to the "Specifications for Wind-Resistant Design Specification for Highway Bridges" (JTG/T 3360-01—2018) [11].

$$[V_{cr}] = \gamma_f \gamma_t \gamma_\alpha V_d \tag{1}$$

The design reference wind speed V_d at deck level is 36.3 m/s for the completed bridge state and 31.9 m/s for the construction state (based on a 20-year return period). Considering a Class B site, the dimensionless correction factor accounting for wind speed fluctuations and horizontal correlation is $\gamma_t = 1.296$. The partial factor for flutter stability is taken as $\gamma_f = 1.25$, and the partial factor for the wind attack angle effect is $\gamma_\alpha = 1.0$. Accordingly, the flutter check wind speed for a 100-year return period is calculated to be 58.8 m/s. For the construction stage, the design reference wind speed at the deck level is 31.9 m/s.

The critical flutter wind speed of long-span bridges can be estimated using the following formula:

$$V_{cr}(\alpha) = \eta_\alpha \eta_s V_{co} \tag{2}$$

where α is the angle of attack, η_α is the wind attack angle correction factor, η_s is the cross-sectional shape correction factor of the bridge, and V_{co} is the flat plate critical flutter speed, which can be calculated using either the Van der Put formula or the Selberg formula as follows.

Van der Put formula:

$$V_{co} = \left(\pi\left[1 + (\varepsilon - 0.5)\sqrt{0.72\mu r/b}\right]/\varepsilon\right) f_t B \tag{3}$$

Selberg formula:

$$V_{co} = 3.71 \left(\sqrt{\frac{m_{eq}r_{eq}}{\rho B^3}[1 - 1/\varepsilon^2]} \right) f_t B \tag{4}$$

where B is the bridge deck width, $\varepsilon = f_t/f_v$ is the torsion-to-bending frequency ratio, f_v is the first vertical bending frequency, f_t is the first torsional frequency, r_{eq} is the equivalent radius of gyration, and μ is the mass density ratio between the structure and the air:

$$r_{eq} = \sqrt{J_{meq}/m_{eq}} \tag{5}$$

$$\mu = m_{eq}/(\pi\rho b^2) \tag{6}$$

Here, m_{eq} and J_{meq} represent the equivalent distributed mass and the distributed mass moment of inertia of the main girder, respectively, considering the overall and spatial vibration characteristics of the bridge. $b = B/2$ is the half-width of the bridge deck.

The combined correction factor for the angle of attack and cross-sectional shape, $\eta_{\alpha s} = \eta_s \eta_\alpha$, is determined on the basis of relevant parameters and critical wind speed test results of bridges with similar cross-sectional profiles:

$$\eta_{\alpha s} = \frac{V_c^r(\alpha)}{V_{co}^r} \tag{7}$$

Finally, on the basis of the parameters of this bridge, the critical flutter wind speed in the completed state is estimated as follows:

$$V_c(\alpha) = \eta_{\alpha s}V_{co} = \frac{V_{co}}{V_{co}^r}V_c^r(\alpha) \tag{8}$$

Table 1 Calculated flutter wind speeds for the two constraint systems

Parameter		Fully Floating	Semi-Floating
Torsional Frequency f_t (Hz)		0.5304	0.5689
Torsion-to-Bending Frequency Ratio ε		1.983	1.979
Equivalent Mass m (kg/m)		4.029E+04	4.18E+04
Equivalent Mass Moment of Inertia J_m (kg·m²/m)		5.071E+06	4.74E+06
Equivalent Radius of Gyration r_{eq} (m)		11.218	10.646
Damping Ratio ξ		0.5	0.5
flat plate critical flutter speed (Van der Put formula) V_{co} (m/s)		200.2	213.3
flat plate critical flutter speed (Selberg formula) V_{co} (m/s)		170.6	181.5
Critical Flutter Wind Speed (Van der Put formula) (m/s)	+3°	70.7	75.3
	0°	105.7	112.6
	-3°	>114.6	>122.1
Critical Flutter Wind Speed (Selberg formula) (m/s)	+3°	69.5	73.9
	0°	103.8	110.4
	-3°	>112.6	>119.7

The estimated minimum critical flutter wind speeds for the two different restraint systems of the bridge (Table 1) provide an approximate evaluation of their flutter stability performance. According to the results, the critical flutter wind speed is 69.5 m/s for the fully floating system and 73.9 m/s for the semi-floating system. In both cases, the critical flutter speeds exceed the required verification wind speed, indicating that the flutter stability requirements are satisfied [12].

3.3 Influence of Tower–Girder Restraint on the Seismic Performance of Self-Anchored Suspension Bridges

A full-bridge finite element model was established in SAP2000 (Figure 8) to analyze and compare the seismic performance of the fully floating and semi-floating restraint systems. The model includes the main span (analysis span) and one approach span on each side as boundary spans. The model incorporates key factors such as foundation springs to simulate pile–soil interactions, bearing elements capable of capturing slippage under seismic loading, additional masses representing actual dead loads, and adjustments to gravitational stiffness due to the initial tension forces in the suspenders.

In the model, the main towers, girders, piers, and pile caps are simulated using beam elements, whereas the suspenders and horizontal tie bars are modeled with truss elements. The geometric stiffness due to the dead load is considered in all the structural elements. The second-stage dead load is applied to the beam elements in the form of a concentrated mass.
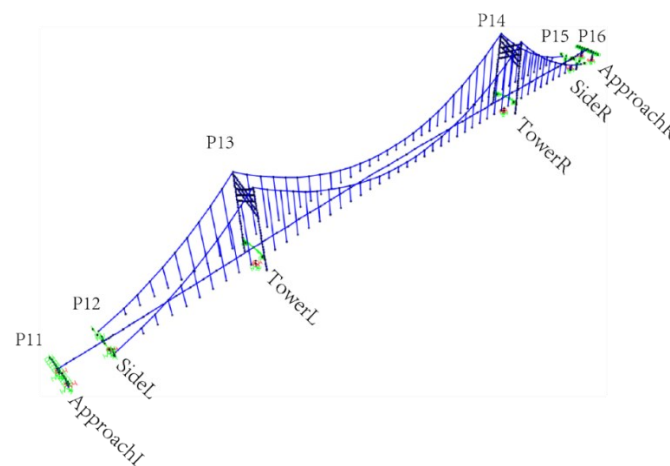

Figure 8 Dynamic analysis model

3.3.1 Analysis and Comparison of Dynamic Characteristics

Analyzing and understanding the dynamic characteristics of bridge structures is fundamental for seismic performance assessment [12–14]. Table 2 presents the first five vibration modes, along with their corresponding periods and mode descriptions, for the two constraint systems. The first mode for both systems corresponds to longitudinal floating of the main girder combined with vertical bending, as illustrated in Figure 9.

By analyzing the first five vibration modes of the fully floating and semi-floating systems, it can be observed that the overall periods of the fully floating system are generally longer—by approximately 3.7%—compared to those of the semi-floating system. Additionally, the occurrence order of the symmetric and antisymmetric vertical bending modes of the main girder is reversed. In the fully floating model, the first symmetric vertical bending mode appears earlier, whereas in the semi-floating model, the first antisymmetric vertical bending mode appears first.
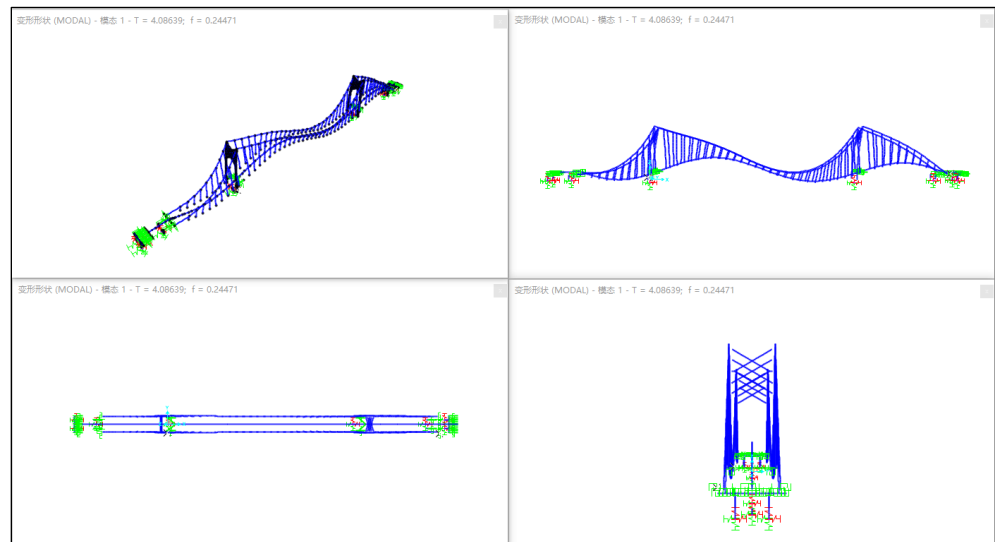
Figure 9 First mode shape of the self-anchored suspension bridge

Table 2 Comparison of mode shapes under two restraint systems

Mode Number	Semi-Floating		Fully Floating	
	Period (s)	Descriptions	Period (s)	Descriptions
1	4.09	Main girder longitudinal swaying + vertical bending	4.24	Main girder longitudinal swaying + vertical bending
2	3.40	1st antisymmetric vertical bending of girder	3.72	1st symmetric vertical bending of girder
3	3.32	1st symmetric vertical bending of girder	3.66	1st antisymmetric vertical bending of girder
4	1.96	1st symmetric in-phase swinging of main cable	2.37	Antisymmetric vertical bending of side spans
5	1.95	Antisymmetric vertical bending of side spans	2.08	2nd symmetric vertical bending of girder

3.3.2 Nonlinear Time History Response Analysis and Comparison

Seven horizontal ground motion records designed from the seismic safety evaluation of the bridge site were applied in both the longitudinal and transverse directions of the bridge, and seven vertical ground motions were combined simultaneously for the time history analysis. The results were averaged to obtain the internal force and displacement responses of the two systems under the E2-level earthquake (with a return period of 2500 years). The results are shown in Figures 10–13.

As shown in Figure 10, under transverse seismic excitation, the internal forces at various sections of the tower in the semi-floating system are reduced, where axial forces decrease by approximately 12–18%, and bending moments and shear forces decrease by approximately 2%. Meanwhile, the shear force and bending moment at the base of the side piers increase, where the bending moment increases by approximately 2%, and the shear force increases by approximately 25%. This is because, under transverse seismic action, the tower behaves approximately like a frame structure, with significant bending moments occurring at both the tower base and the upper crossbeam. In the semi-floating system, the bearings placed at the corbels provide certain lateral stiffness from the girder to the tower, thereby affecting the distribution of transverse forces.
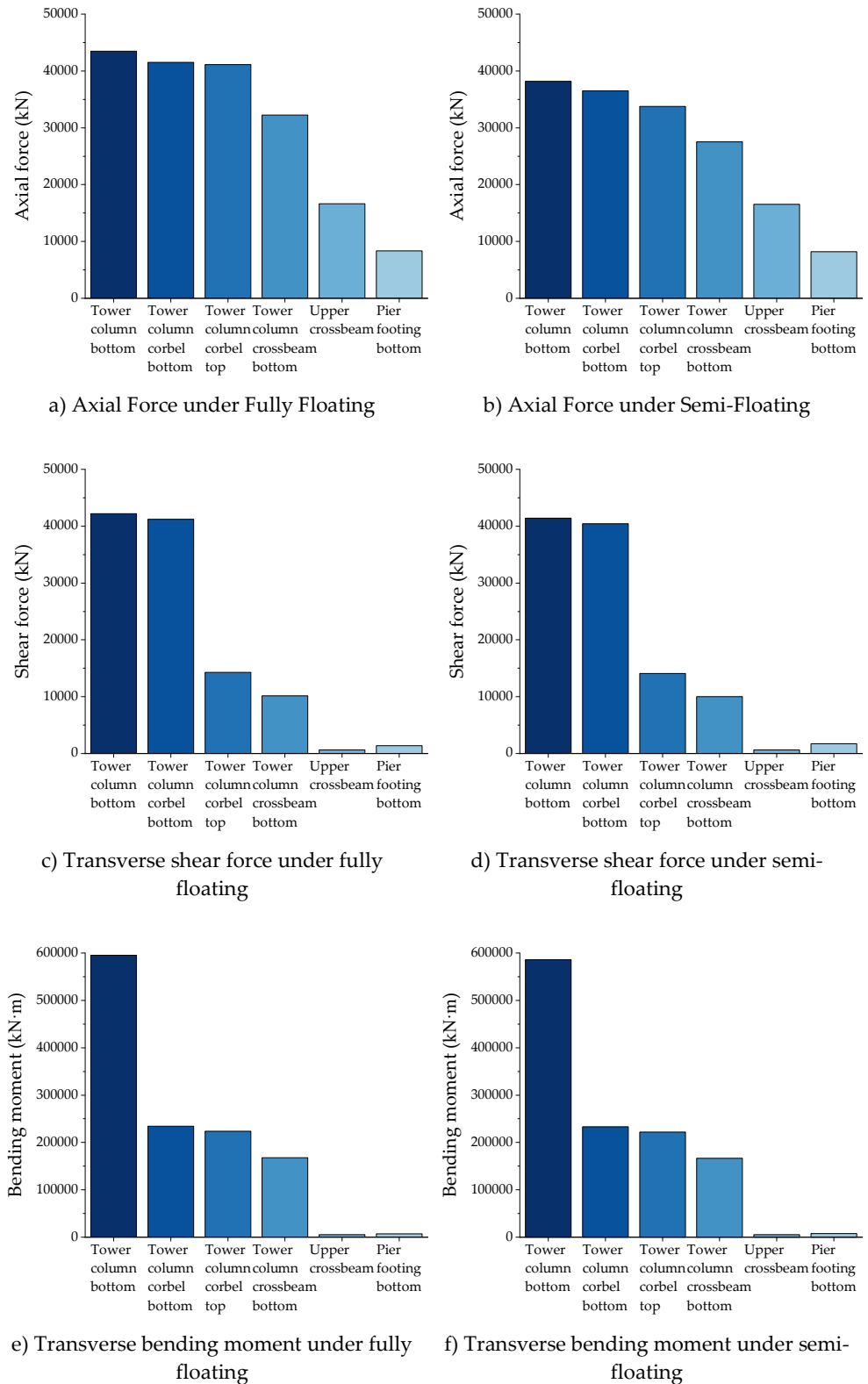
a) Axial Force under Fully Floating

b) Axial Force under Semi-Floating

c) Transverse shear force under fully floating

d) Transverse shear force under semi-floating

e) Transverse bending moment under fully floating

f) Transverse bending moment under semi-floating

Figure 10   Internal forces at key sections under transverse seismic action (E2)

Figure 11 shows that under longitudinal seismic action, the dynamic axial forces at various sections of the bridge tower in the semi-floating system are reduced by approximately 16% to 27%, whereas the dynamic bending moments increase by approximately 3%. The shear forces and bending moments at the base of the side piers show little variation.
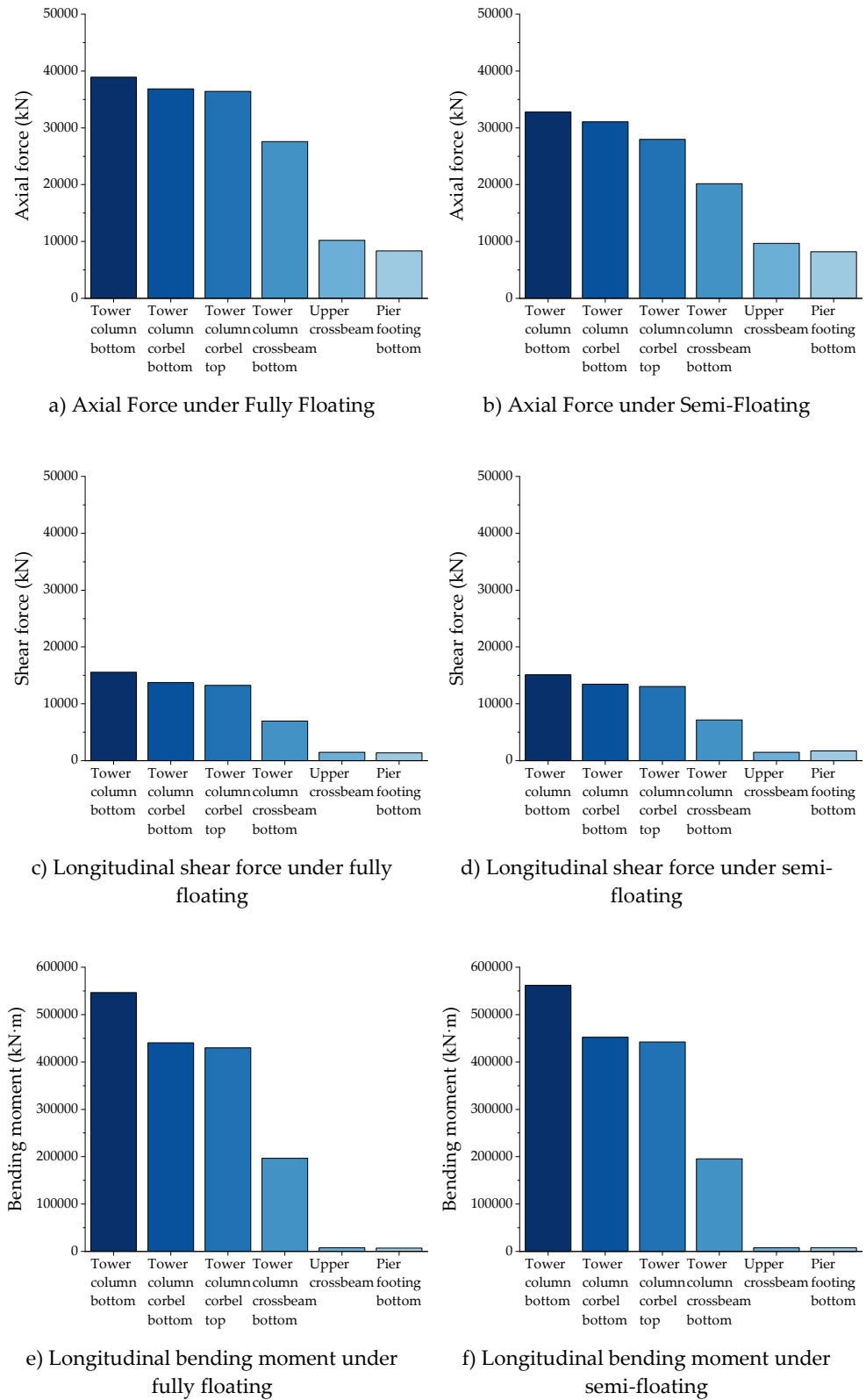
a) Axial Force under Fully Floating

b) Axial Force under Semi-Floating

c) Longitudinal shear force under fully floating

d) Longitudinal shear force under semi-floating

e) Longitudinal bending moment under fully floating

f) Longitudinal bending moment under semi-floating

Figure 11   Internal forces at key sections under longitudinal seismic action (E2)

Figure 12 shows that the foundation reactions at the side piers and the base shear force and bending moment at the main tower are similar for both systems. In contrast, the dynamic axial force at the main tower base in the fully floating system is approximately 4% greater than that in the semi-floating system.
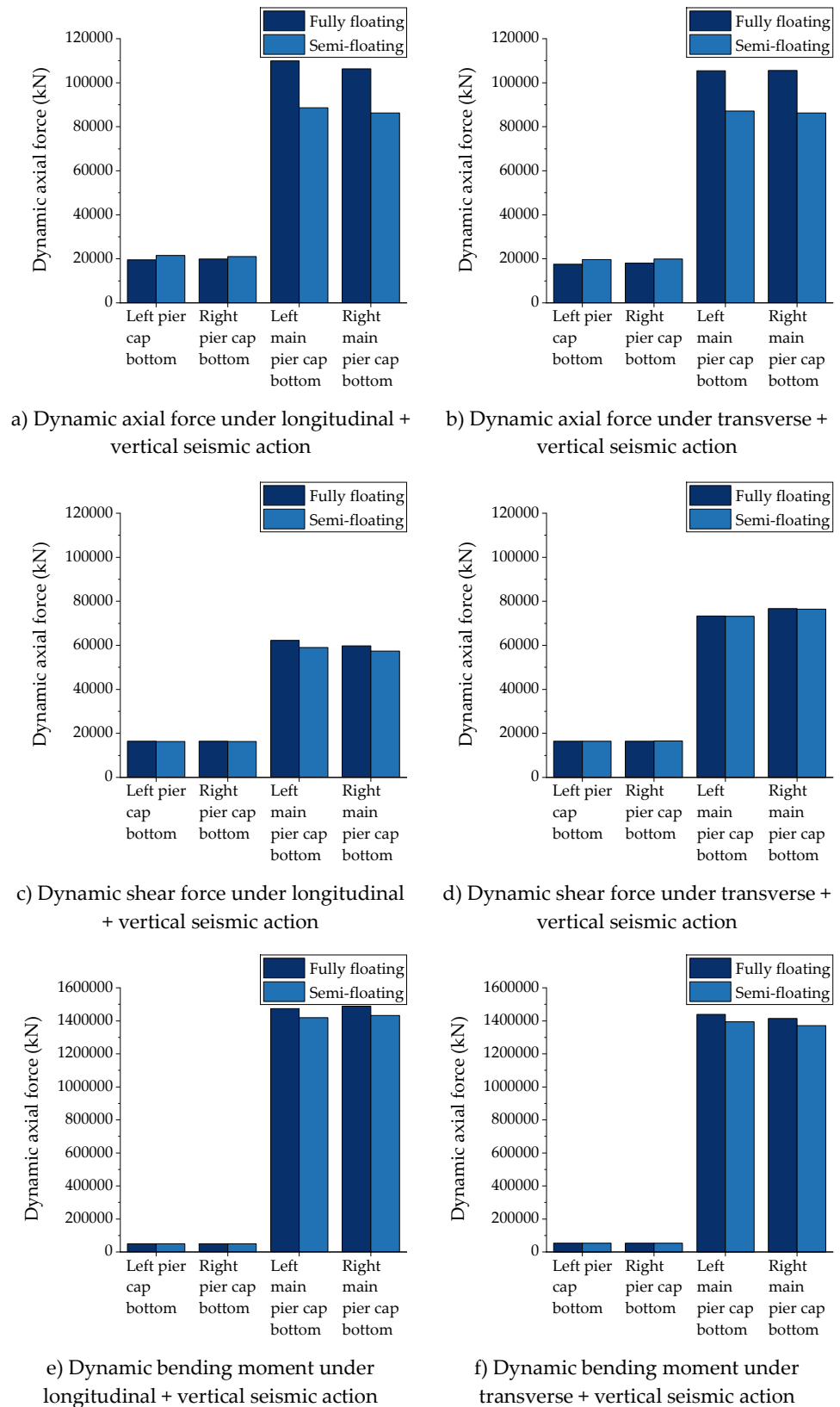
a) Dynamic axial force under longitudinal +
vertical seismic action

b) Dynamic axial force under transverse +
vertical seismic action

c) Dynamic shear force under longitudinal
+ vertical seismic action

d) Dynamic shear force under transverse +
vertical seismic action

e) Dynamic bending moment under
longitudinal + vertical seismic action

f) Dynamic bending moment under
transverse + vertical seismic action

Figure 12   Foundation reactions under seismic action (E2)

Figure 13 shows the longitudinal and transverse displacements of the main girder under seismic action for both structural systems. The results indicate that the longitudinal displacement of the main girder differs only slightly between the two systems, with the semi-floating system exhibiting a slightly smaller value—approximately 7% lower.
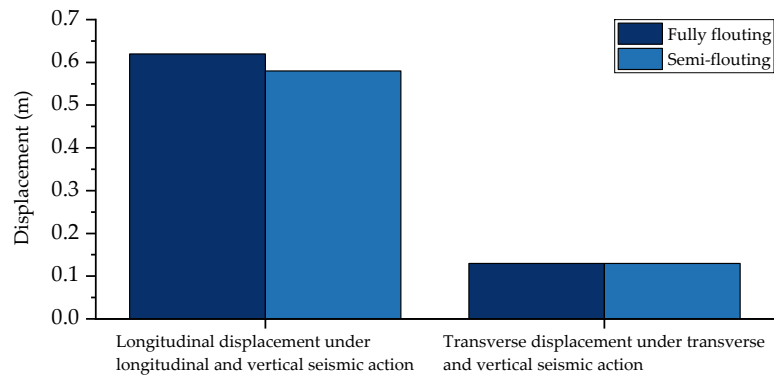
Figure 13   Displacement of the main girder under seismic action (E2)

In general, the structural period of the fully floating system tends to be longer than that of the semi-floating system. However, for this self-anchored suspension bridge, the stiffness around the tower area is relatively high because of the installation of stoppers and transverse bearings on both sides of the main girder, resulting in only a minor increase in the structural period. With respect to the seismic response, the internal forces in the tower columns and base reactions are greater in the fully floating system. This is mainly because the vertical vibration mode appears earlier in the fully floating configuration. In the semi-floating system, part of the vertical and longitudinal inertial forces of the main girder are transmitted to the tower through the corbels via friction. In contrast, in the fully floating system, the vertical support at the tower location is removed. Consequently, the inertial forces of the main girder are transferred to the top of the tower via the hangers, increasing the force arm and leading to higher internal forces in the tower and larger base reactions. The fully floating system has a slight effect on the longitudinal displacement of the bearings at the side piers, with an increase of approximately 7%. The longitudinal displacement at the bearings near the main towers is approximately 0.6 m for both systems.

4   Conclusions

Taking a self-anchored suspension bridge as the research subject, finite element analysis software was employed to investigate the structural performance under two different constraint systems: the fully floating system and the semi-floating system. The static, aerodynamic, and seismic behaviors of the bridge were analyzed, leading to the following conclusions:

(1)   Under a live load, the bending moment envelopes of the main girder across most regions of the bridge show minimal differences between the two systems. However, the tower–girder constraint has a more significant effect on the local bending moments of the main girder near the supports, with the semi-floating system exhibiting notably larger moments at the support locations. The maximum live-load deflection of the main girder in the semi-floating system is slightly smaller than that in the fully floating system. Both systems have some influence on live-load deflection, but the effect is not substantial. For both constraint systems, the first global instability mode of the bridge corresponds to tower instability. The difference in the stability coefficients between the two systems is minor, with the semi-floating system having a slightly higher stability coefficient.

(2)   The flutter critical wind speeds of both systems exceed the flutter checking wind speed, with the semi-floating system providing a slightly greater safety margin.

(3) Compared with the semi-floating system, the floating system shows a 3.7% increase in the longitudinal drift period of the main girder and a 7.2%–21.5% increase in the vertical bending period. However, the oscillation modes of the main cable of both systems are basically consistent. Additionally, owing to the different constraints on the main girder at the tower location in the two models, the floating system exhibits earlier occurrence of side-span antisymmetric vertical bending and second-order symmetric vertical bending modes of the main girder.

(4) In terms of the vertical seismic response, the floating system leads to increased seismic axial forces in the tower columns and pile foundations, resulting in reduced bending resistance, which is unfavorable for seismic performance. Moreover, the floating system has a slight impact on the longitudinal displacement of the bearings at the side piers. Both systems exhibit large longitudinal displacements at the tower bearings, making it challenging to select suitable expansion joints and necessitating the adoption of seismic mitigation measures.

References

1. Zhang, Z.; Dou, P.; Shi, L.; Liu, C. A Review of the Development of Self-Anchored Suspension Bridges. *World Bridges* **2003**, 1, 5-9.
2. Ochsendorf, J. A.; Billington, D.P. Self -Anchored Suspension Bridges. *J. Bridge Eng.* **1991**, 4, 155.
3. Zhang, Y.; Dai, J.; Shao, C. Key Design Techniques for Egongyan Railway Transit Bridge. *Bridge Constr.* **2020**, 50(4), 82-87. https://doi.org/10.3969/j.issn.1003-4722.2020.04.014
4. Hu, S.; Fan, L. The Longitudinal Earthquake Response Analysis for the Jiangyin Yangtze River Bridge. *J. Tongji Univ. Nat. Sci.* **1994**, 22(4), 433-438.
5. Huang, K. Analysis of Travelling Wave Effects on Large Span Suspension Bridge. *Technol. Highw. Transp.* **2020**, 36(2), 70-74. https://doi.org/10.13607/j.cnki.gljt.2020.02.011
6. Li, C. Dynamic Analysis of Long-Span Pedestrian Suspension Bridge. Degree of Master, Central South University of Forestry & Technology, Changsha, 2019.
7. Wu, K. Study on Dynamic Characteristics of Long-Span Suspension Bridge and Its Parametric Analysis. Degree of Master, Changsha University of Science & Technology, Changsha, 2007. https://doi.org/10.7666/d.y1189015
8. Feng, G. Structure Static Characteristics Analysis of Long Span Suspension Bridge with Double Main Cable. Degree of Master, Beijing Jiaotong University, Beijing, 2019.
9. Liu, J.; Wang, H.; Yao, J.; Huang, K.; Lan, W.; Han, T. Design and Research on Constraint Conditions Between Main Tower and Main Girder of Suspension Bridge. *Road Mach. Constr. Mech.* **2020**, 37, 31-34.
10. Ministry of Transport of the People's Republic of China JTG/T D60—2015, General Code for Design of Highway Bridges and Culverts. China Communications Press: Beijing, 2015.
11. Ministry of Transport of the People's Republic of China JTG/T 3360-01—2018, Wind-resistant Design Specification for Highway Bridges. China Communications Press: Beijing, 2018.
12. Chen, Y. Experimental Study on Wind Resistance Performance of Semi-closed Box Girder of Long-span Self-anchored Suspension Bridge. *Eng. Technol. Res.* **2024**, 6, 1-4. https://doi.org/10.19537/j.cnki.2096-2789.2024.06.001
13. Kang, J.; Yuan, M.; Wang, T. Parametric Analysis of Dynamic Performance of Completion State of Long Span Self-Anchored Suspension Bridge. *Bridge Constr.* **2013**, 43(6), 64-70.

14.   Li, Z.; Han, X.; Li, A.; Miao, C.; Feng, Z. Dynamic Analysis and Test of Bridge Tower of Suspension Bridge Before and After Cable Installed. *Chin. J. Highw. Transp.* **2007**, 20(5), 54-58. https://doi.org/10.3321/j.issn:1001-7372.2007.05.010

AUTHOR BIOGRAPHIES

	Changyan Niu M.E., Senior Engineer. Graduated from Tongji University in 2006. Working at Shanghai Municipal Engineering Design Institute (Group) Co., Ltd. Research Direction: Design of Bridge Structure. Email: niuchangyan@smedi.com		**Yongcheng Lu** B.E., Prof. Engineer. Graduated from Shanghai Institute of Urban Construction college in 1986. Working at Shanghai Municipal Engineering Design Institute (Group) Co., Ltd. Research Direction: Design of Bridge Structure. Email: luyongcheng@smedi.com
	Jianguo Dai M.E., Prof. Engineer. Graduated from Tongji University in 1999. Working at Shanghai Municipal Engineering Design Institute (Group) Co., Ltd. Research Direction: Design of Bridge Structure. Email: daijianguo@smedi.com		